Excitations in $KCoF_3$-I. Experimental

1971 J. Phys. C: Solid State Phys. 4 2127

(http://iopscience.iop.org/0022-3719/4/14/027)

J. Phys. C: Solid St. Phys., 1971, Vol. 4. Printed in Great Britain

Excitations in $KCoF_3$—I. Experimental

T. M. HOLDEN†, W. J. L. BUYERS†, E. C. SVENSSON†, R. A. COWLEY†, M. T. HUTCHINGS‡§, D. HUKIN‡ and R. W. H. STEVENSON¶

† Atomic Energy of Canada Limited, Chalk River, Ontario, Canada
‡ Clarendon Laboratory, Oxford University, Oxford
¶ Department of Natural Philosophy, The University, Aberdeen, Scotland

MS. received 24th November 1970

Abstract. Dispersion curves for magnons and phonons propagating in $KCoF_3$ at low temperatures have been determined by means of neutron inelastic scattering techniques. Two branches of magnetic excitations have been observed corresponding to a transition between the two members of the ground state doublet ($j = \frac{1}{2}$) of the Co^{2+} ion and a transition between the ground state and the lowest member of the $j = \frac{3}{2}$ spin–orbit level. Neither branch shows evidence for the directional anisotropy which has been suggested for the exchange interactions in $KCoF_3$; any splitting of the doubly degenerate magnon branch is shown to be less than 8% in frequency. The magnon branch of lowest frequency interacts with a phonon branch in the vicinity of the magnetic zone centre. The strength of the magnon–phonon interaction is found to be $0{\cdot}35 \pm 0{\cdot}10$ THz and from the temperature dependence of the modes the magnon–phonon interaction is shown to be appreciable only within a radius $0{\cdot}2 \times 2\pi/a$ of the magnetic zone centre. The magnetic modes of higher frequency show a marked decrease in intensity with increasing temperature but little change in frequency in accordance with expectations for a transition that depends strongly on the spin–orbit coupling but only weakly on the exchange.

1. Introduction

The spin wave dispersion relations of several magnetic iron group compounds, namely MnF_2 (Okazaki *et al.* 1964), MnO (Collins 1964), $RbMnF_3$ (Windsor and Stevenson 1966), $KMnF_3$ (Pickart *et al.* 1966), CoF_2 (Martel *et al.* 1968), FeF_2 (Hutchings *et al.* 1970a), CoO (Sakurai *et al.* 1968), Cr_2O_3 (Samuelson *et al.* 1970), NiF_2 (Hutchings *et al.* 1970b), Fe_2O_3 (Samuelson and Shirane 1970), have now been determined by the technique of neutron inelastic scattering. Because the orbital angular momentum of the Co^{2+} ion is not quenched by the crystal field, the materials containing Co^{2+} ions exhibit several features which are different from those of the other materials.

The orbital angular momentum gives rise to the possibility that the excited states have sufficiently low energies for there to be considerable mixing of the states by the exchange field. The exciton modes associated with these excited states may also have energies which are readily accessible in neutron scattering experiments. In this experiment the two branches of the magnetic excitations of lowest frequency have been studied. The finite orbital angular momentum is associated with an anisotropic spatial distribution of the magnetic electrons of the Co^{2+} ions. The anisotropy can lead to an anisotropic exchange energy between pairs of ions but the present results (§ 3.2) show that any anisotropy is quite small for $KCoF_3$ and that the exchange is predominantly of the well known Heisenberg form. The orbital angular momentum may also lead to interaction between the magnons and the phonons; this has been observed (§ 3.3) in $KCoF_3$ and its magnitude obtained. In earlier studies of CoF_2 (Martel *et al.* 1968) and CoO (Sakurai *et al.* 1968) some of the above features had been apparent, but since $KCoF_3$ has a much simpler crystal structure than CoF_2 and a much

§ Now at AERE Harwell, Didcot, Berkshire.

simpler magnetic structure than CoO, it was hoped, and indeed it proved to be true, that the interpretation of measurements on $KCoF_3$ would be more straightforward.

The experimental measurements and results are discussed in this paper and the paper which follows (Buyers *et al.* 1971, to be referred to as II) deals with the theoretical analysis of the results. A preliminary account of this study was given earlier (Buyers *et al.* 1968).

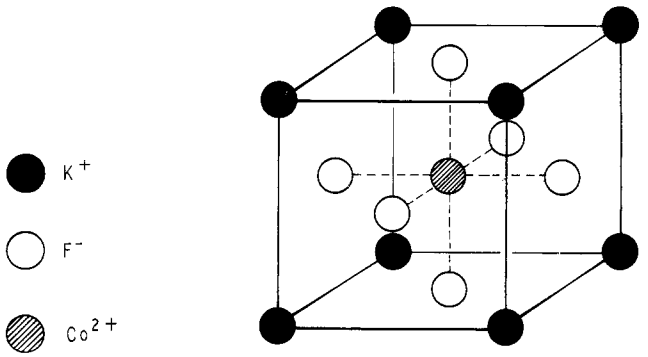

Figure 1. The crystal structure of $KCoF_3$.

$KCoF_3$ has the cubic perovskite structure (figure 1) in the paramagnetic phase (Okazaki and Suemune 1961). Below $T_N = 114$ K, the magnetic moment on a cobalt ion points along a cube edge, and each cobalt ion is antiferromagnetically coupled to its six nearest cobalt neighbours (Scatturin *et al.* 1961). A small tetragonal distortion (0·2% in the lattice parameter at 78 K) accompanies the magnetic ordering (Okazaki and Suemune 1961). In

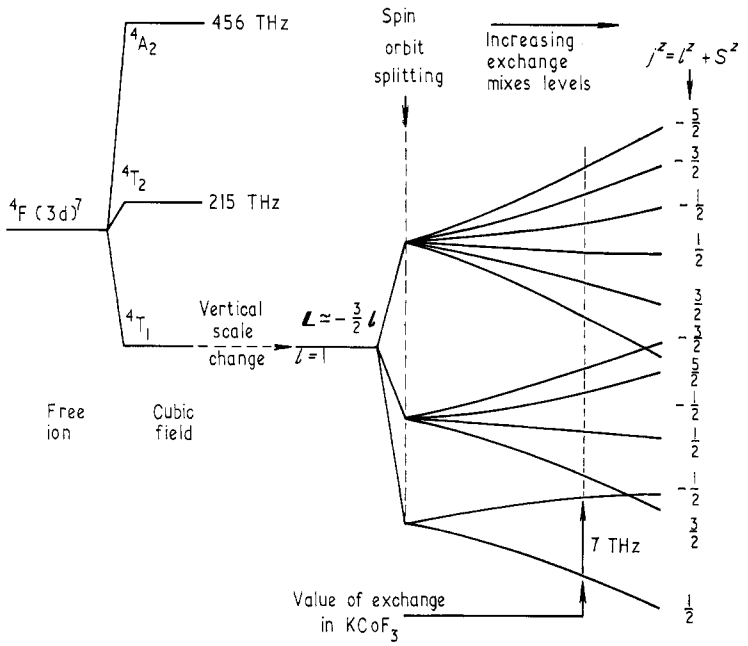

Figure 2. The energy level diagram of Co^{2+} ions in $KCoF_3$ showing the effects of the cubic crystalline field, spin–orbit interaction and the exchange field. The effect of the tetragonal distortion of $KCoF_3$ is too small to be shown on this scale.

general there will be three possible orientations of the antiferromagnetic domains corresponding to the directions of the cube edges, and these should be populated about equally in an experiment, such as this one, where no special precautions are taken to align the domains. In the absence of directional interactions (see § 3.2) the frequencies will be the same in each domain.

At this point it is useful to consider the energy level scheme (figure 2) of the cobalt ion in $KCoF_3$. The ground state of the free Co^{2+} ion has a total orbital angular momentum $L = 3$ and total spin $S = \frac{3}{2}$. This ^4F state is split by the octahedral crystal field provided by the fluorine neighbours to give an orbital singlet and two orbital triplet states. The lowest state, the triplet $^4T_1$, is separated from the next higher state $^4T_2$ by approximately 215 THz (Ferguson *et al.* 1963) which is well beyond the energy range accessible to neutron inelastic scattering. (The unit THz $= 10^{12}$ Hz, which will be used throughout this paper, is equivalent to 48·0 K, 4·14 meV or 33·3 cm^{-1}.) The $^4T_1$ orbital triplet has the same symmetry as a manifold of p states and can be described as an effective $l = 1$ state. Spin–orbit coupling in the cubic crystal field then splits the $l = 1$ state to give multiplets characterized by the values of $j = l + S$. Finally the exchange field in the antiferromagnetic phase mixes and splits these multiplets to produce twelve levels characterized by values of $j^z = l^z + S^z$. Excitations corresponding to transitions between the ground state and the first and second excited states have been studied in the present experiment. In order to describe the way in which these excitations propagate through the crystal, a spin wave theory is required and this subsequently permits the determination of the exchange interactions between the ions. These topics are dealt with in detail in II. Details of the experiment are given in § 2. The results of the measurements are presented and discussed in § 3.

2. Experimental details

2.1. *Neutron scattering and the reciprocal lattice*

For the present study, the processes of primary interest are those in which a neutron is scattered with the creation or annihilation of one quantum of energy. The conditions of conservation of energy and momentum for such processes are

$$E_0 - E' = \pm h\nu_j(\boldsymbol{q}) \tag{1}$$

and

$$\boldsymbol{k}_0 - \boldsymbol{k}' = \boldsymbol{Q} = 2\pi\boldsymbol{\tau} + \boldsymbol{q}. \tag{2}$$

$E_0(E')$ and $\boldsymbol{k}_0(\boldsymbol{k}')$ are the incident (scattered) neutron energy and wavevector, $\boldsymbol{Q}$ is the wavevector transfer, $\boldsymbol{\tau}$ is a reciprocal lattice vector, and $h\nu_j(\boldsymbol{q})$ and $\boldsymbol{q}$ are the energy and wavevector of the excitation (j is a branch index).

The (110) plane of the reciprocal lattice of $KCoF_3$ is shown in figure 3. The Brillouin zone for the chemical unit cell, which is the one relevant for the lattice vibrations, is shown by broken lines. In the antiferromagnetic phase, magnetic Bragg reflections occur at points such as $(\frac{1}{2}\,\frac{1}{2}\,\frac{1}{2})$ and $(\frac{1}{2}\,\frac{1}{2}\,\frac{3}{2})$ which have half integral indices in the normal scheme for labelling the nuclear Bragg reflections. The Brillouin zones relevant for magnetic excitations are shown as full lines in figure 3. For the case of a simple two-sublattice spin-only antiferromagnet considered by Nagai and Yoshimori (1961), the intensity of scattering by spin waves is greatest in magnetic Brillouin zones containing magnetic reciprocal lattice points.

It is also possible to observe the lattice vibrations via the magnetic interaction of the neutron instead of via the nuclear interaction. Such scattering is known as magnetovibrational scattering and at low temperatures the cross section is essentially that for phonons with the nuclear scattering length replaced by the magnetic scattering length. The Brillouin zone for magnetovibrational scattering is the same as the chemical Brillouin zone (broken lines in figure 3) but centred on a magnetic reciprocal lattice point. Magnetovibrational scattering will only occur, of course, for lattice vibrational modes which involve motions of the magnetic ions.

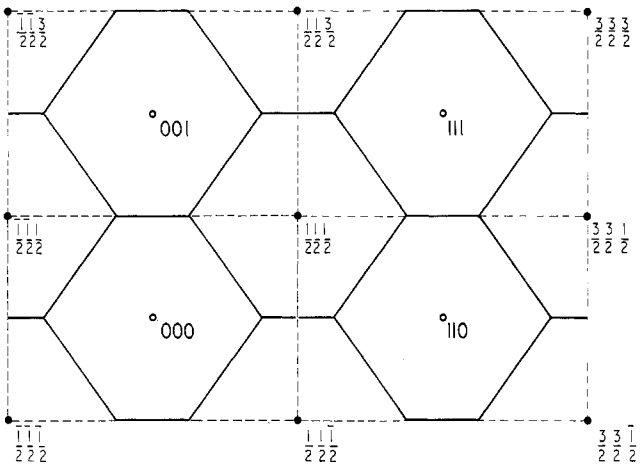

Figure 3. The $(1\bar{1}0)$ plane of the reciprocal lattice of $KCoF_3$. Full (open) circles indicate magnetic (nuclear) reciprocal lattice points and full (broken) lines indicate magnetic (chemical) Brillouin zones.

2.2. *Instruments*

The measurements were carried out using the phased-chopper spectrometer (Dyer and Low 1961) at the PLUTO reactor (Harwell), a triple-axis crystal spectrometer at the DIDO reactor (Harwell), and a triple-axis crystal spectrometer at the NRU reactor (Chalk River). The triple-axis spectrometers were operated in the constant momentum transfer (constant $\boldsymbol{Q}$) mode (Brockhouse 1961). In time-of-flight measurements the energy distribution of scattered neutrons is deduced from the arrival time spectrum of the neutrons at a fixed counter for a fixed sample orientation. The momentum transfer $\boldsymbol{Q}$ (and hence $\boldsymbol{q}$) varies through the distribution.

2.3. *Specimens*

Two different specimens were studied in these experiments. Specimen A, of volume 3 cm^3, was used for the time-of-flight and triple-axis crystal spectrometer measurements at Harwell, where it was aligned so that the $(1\bar{1}0)$ axis was normal to the scattering plane. For subsequent measurements at Chalk River, A was aligned so that a $(11\bar{2})$ axis was normal to the scattering plane. Specimen B consisted of two single crystals of total volume 4 cm^3. The two crystals were aligned so as to have a common crystallographic orientation with a $(1\bar{1}0)$ axis normal to the scattering plane. Specimen B was used for the majority of the measurements at Chalk River. The method of crystal growth has already been described (Svensson *et al.* 1969).

The specimens were mounted in helium cryostats and the temperatures were controlled by heaters operating in conjunction with platinum and germanium resistance thermometers.

3. Results and discussion

3.1. *The dispersion relations*

The experimental frequencies for magnons and phonons in $KCoF_3$ at low temperatures (<22 K) are summarized in figures 4 and 5. The results obtained with the triple-axis crystal spectrometers at Chalk River and at Harwell are shown in figure 4 by circles and triangles respectively. The results obtained with the time-of-flight spectrometer for excitations propagating along the $[0, 0, \zeta]$ direction are shown in figure 5 as squares. The scatter in the latter results arises at least partly because the measurements could not be carried out at preselected wavevectors, and the results shown are those lying within 5° of the $[0, 0, \zeta]$

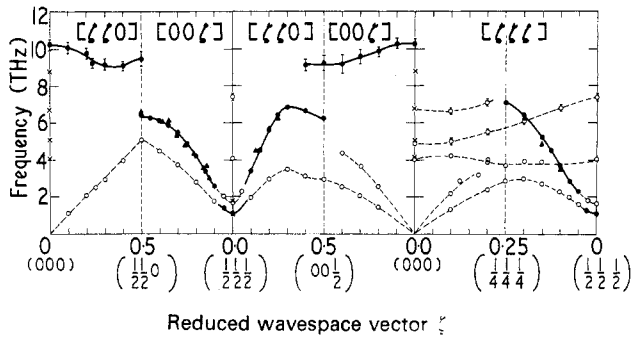

Figure 4. The dispersion curves for excitations in $KCoF_3$ at low temperatures. Full (open) symbols and full (broken) curves indicate excitations of a predominantly magnetic (phonon) character. The lines are intended as guides to the eye. Circles and triangles show the results of crystal spectrometer measurements made at Chalk River and Harwell respectively. Crosses show the results of measurements by optical techniques. Wave vectors, specified by ζ in units of $2\pi/a$, are appropriate to the magnetic Brillouin zone. Reciprocal space coordinates are indicated at the bottom of the figure.

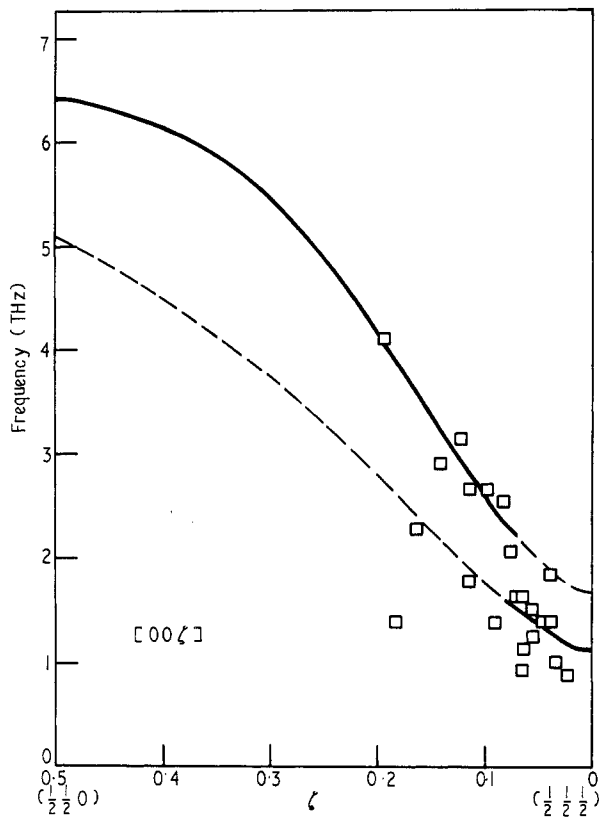

Figure 5. The dispersion curve for excitations propagating in the [00ζ] direction in $KCoF_3$. Squares denotes measurements made with the time-of-flight spectrometer.

direction. Figure 5 is typical of the time-of-flight results which, for the other directions also, are in agreement with the triple-axis spectrometer results but are less accurate.

The character of the excitations is indicated in figure 4 by using full (open) symbols to denote those excitations of a predominantly magnetic (lattice vibrational) character. The evidence for this assignment will be presented in §§ 3.3 and 3.4 where the effect of temperature is discussed.

Table 1. Comparison of excitation frequencies (THz) observed in the present neutron scattering experiment at the magnetic zone centre with frequencies observed in infrared experiments

Mode	Neutron scattering	Infrared (1)	(2)	(3)
Magnon†	1·12 ± 0·06	1·11 ± 0·01		
TA phonon†	1·69 ± 0·05	1·72 ± 0·01		
TO phonon	4·07 ± 0·08	4·11	4·16	4·20
LO phonon	4·90 ± 0·16	5·11	5·05	4·68
TO phonon			6·75	6·72
LO phonon			8·8	8·8
Magnon	10·25 ± 0·3			
TO phonon			12·5	12·9
LO phonon			15·0	15·3

(1) Phillips 1968, (2) Axe and Pettit 1967, (3) Perry and Young 1967.
† Modes affected by magnon–phonon interaction and having partially mixed character.

The frequencies of modes observed at the centres of magnetic Brillouin zones are listed in table 1 where they are compared with the results of optical and infrared measurements. The agreement is excellent. Some results obtained using the time-of-flight spectrometer did suggest the presence of a mode at approximately 0·7 THz. T. G. Phillips (1968 private communication) has also observed a mode having a frequency of 0·68 ± 0·01 THz which is independent of magnetic field. Extensive searches carried out using the triple-axis crystal spectrometers, however, gave no evidence for such a low frequency mode in either specimen A or specimen B.

In figure 4 the results for the phonon branch between (0·3, 0·3, 0·5) and (0, 0, 0·5) and all the phonon branches in the $[\zeta\zeta\zeta]$ direction except the TA branch were taken from measurements carried out at 150 K. (Except in the region of the magnon–phonon interaction, the phonon frequencies are not expected to be very temperature dependent between 4·2 K and 150 K.)

The study of phonons in $KCoF_3$ is considerably more difficult than the study of magnons because of the low scattering cross section for phonons and the complexity of the phonon dispersion relation. Except for the lowest TA phonon branch the phonon measurements can be regarded as of secondary importance for the purposes of the present paper and no theoretical interpretation of the phonon spectra is given. The broken curves in figure 4 show the probable continuity of the modes.

3.2. *Directional isotropy of the exchange interaction.*

The theory of superexchange (Anderson 1963) indicates that the form of the exchange interaction between ions having orbital angular momentum should be more complex than the isotropic Heisenberg–Dirac exchange (Van Vleck 1932) which has been found to describe spin-only systems such as MnF_2 (Okazaki *et al.* 1964) and $KMnF_3$ (Pickart *et al.* 1966). Elliott and Thorpe (1968) have shown that for $KCoF_3$ the theory predicts an exchange interaction that is anisotropic along the bond joining two Co^{2+} ions. In II it is shown that this leads to a splitting of the magnon dispersion curves whose magnitude is determined by

the anisotropy in the exchange. In contrast to these predictions, no splitting has been observed in this experiment for any of the magnons belonging to the two branches of lowest frequency. From the results for the mode at the [00ζ] zone boundary (figure 6(*a*)) we can say that if a splitting exists it is within the experimental resolution and does not exceed 0·5 THz or 8%.

The dispersion curves for the lower magnon branch in figure 4 exhibit a simple form similar to that observed for spin-only systems with nearest neighbour interactions; for example the [00ζ] and [ζζ0] zone boundary spin wave frequencies are practically the same. One might qualitatively conclude that the exchange has a simple form and this is borne out by the calculation (II) of the complete set of magnetic excitations which shows that the results are consistent with an isotropic exchange interaction. The anisotropy gap at $\boldsymbol{q} = 0$ is a result of the crystal field acting on the orbital angular momentum.

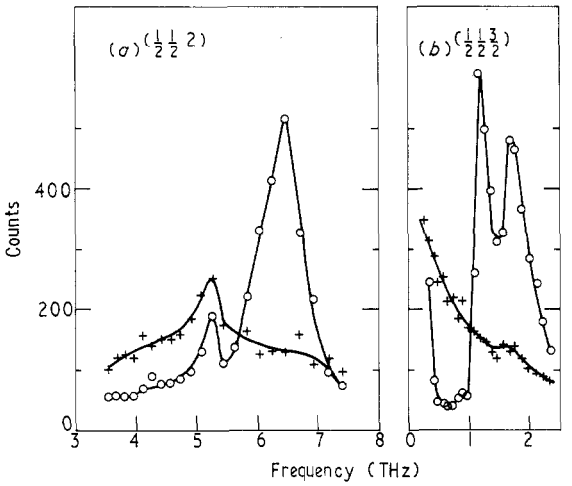

Figure 6. Scattered neutron distributions obtained in 'constant $\boldsymbol{Q}$' experiments (*a*) at the [00ζ] zone boundary and (*b*) at the centre of the magnetic Brillouin zone. The wavevectors are in units of $2\pi/a$. Circles, 20 K; crosses, 120 K.

3.3. *The magnon–phonon interaction*

In this section a description is given of the magnon–phonon interaction observed near the centre of the magnetic zone and how the magnon or phonon character of the modes is established. The method for distinguishing between magnons and phonons depends on the fact that at temperatures lower than T_N the magnon frequencies are much more temperature dependent than the phonon frequencies. The scattered neutron distributions obtained in 'constant $\boldsymbol{Q}$' measurements at the [00ζ] zone boundary position and at the centre of the magnetic Brillouin zone are shown in figure 6. At the [00ζ] zone boundary (figure 6(*a*)), the mode of higher frequency at 20 K is essentially absent above T_N while the lower frequency mode is essentially unchanged. Hence at this wavevector, the modes of higher and lower frequency at low temperatures are probably pure magnon and pure phonon respectively. At the centre of the magnetic zone (figure 6(*b*)), however, the situation is almost reversed. At 120 K there is a broad paramagnetic scattering distribution and a weak peak at a frequency slightly lower than that of the higher mode at 20 K. These results and the results of measurements at intermediate and higher temperatures indicate that, at the zone centre, the modes of lower (higher) frequency at low temperatures have mainly magnon (phonon) character. The partial magnetic character of the higher frequency mode (Phillips 1968 private communication) probably accounts for its intensity being much greater at 20 K than at 120 K.

The fact that there is a reversal in the character of the upper and lower modes between the zone centre and the zone boundary (figure 6) without the branches crossing (figure 4) indicates that there is a magnon–phonon interaction. The strength of the magnon–phonon interaction may most easily be obtained by constructing magnon and phonon dispersion curves as they would be in the absence of the interaction. The splitting of the observed excitations at the crossover of the 'pure magnon' and 'pure phonon' branches then gives the magnon–phonon interaction constant. A further advantage of this procedure is that the 'pure magnon' branch may then be directly compared with the results of spin wave theory.

By assuming that the observed modes at the magnetic zone centre and the zone boundaries were essentially pure modes, the 'pure magnon' branch for each of the three principal symmetry directions was constructed by drawing a smooth curve from the lower mode at the zone centre to the upper mode at the zone boundary. Guided by the study of the temperature dependence of the modes (§ 3.4) the boundary of the region of mixed magnon–phonon character was taken to be at a radius of 0·3 Å^{-1} from the magnetic zone centre. The 'pure phonon' curve was similarly constructed by joining the upper mode at the zone centre to the lower mode at the zone boundary. The zone centre frequencies were taken from the work of Phillips (see table 1).

The 'pure magnon' and 'pure phonon' curves that result from the above procedure (see figure 4 of II) although somewhat subjective are probably accurate to 0·1 THz near the crossover point. The main weakness in the method is the assumption of pure modes at the magnetic zone centre.

The magnon–phonon interaction coefficient ϵ is then normally equal to half the splitting between the observed excitations at the crossover of the 'pure magnon' and 'pure phonon' dispersion curves (Kittel 1963). In $KCoF_3$ the situation is more complex because, even at the centre of the magnetic zone, the interaction takes place between the doubly degenerate magnon modes and two members of the Γ_{25} phonon mode. Although the observed splitting 2ϵ is now $\sqrt{2}$ times the interaction coefficient (see II) we shall nevertheless give ϵ as a measure of the strength of the interaction. From the pure magnon and phonon dispersion curves the crossover point is found to be at a radius of $(0{\cdot}07 \pm 0{\cdot}03)\, 2\pi/a$ from the magnetic zone centre in all three symmetry directions. The mean value of ϵ obtained in this way is $0{\cdot}35 \pm 0{\cdot}10$ THz.

In order to develop a theory of the magnon–phonon interaction (see II), it is necessary to know the phonon eigenvectors. Since the crossover point is very close to the magnetic zone centre (ie the $[\zeta\zeta\zeta]$ zone boundary of the chemical Brillouin zone), we assume that the eigenvectors at the crossover point are the same as those at this zone boundary and the latter can be found once the irreducible representation of the interacting phonon mode is known. It is believed that the correct assignment of the mode is Γ_{25} because this is consistent with the measured intensities in our experiments and with the compatibility relationships. Furthermore it is known that the mode of lowest frequency at the $[\zeta\zeta\zeta]$ zone boundary in $KMnF_3$ (Minkiewicz and Shirane 1969) is Γ_{25} and the phonon dispersion curves of $KMnF_3$ and $KCoF_3$ and their alloys (Buyers *et al.* 1970) are very similar as shown in figure 7. The identification of this mode as Γ_{25} then gives the eigenvectors of the mode unambiguously (Cowley 1964).

3.4. *Temperature dependence of the low frequency magnons and phonons*

The temperature dependence of the spin waves and phonons propagating along the $[00\zeta]$ direction in the antiferromagnetic phase was studied in detail in order to establish the region of reciprocal space over which the magnon–phonon interaction causes a mixing of the modes. Figure 8 shows the temperature dependence of the frequency and width at half height of the two lowest branches at a series of wavevectors. From $\zeta = 0{\cdot}5$ to $\zeta = 0{\cdot}2$ the frequency of the upper mode falls as the temperature increases and the linewidth of the observed neutron group increases. The frequency and linewidth of the lower mode, however, remain essentially constant below T_N and the frequency shows a slight tendency to increase above T_N. In this region the magnon (phonon) character of the upper (lower) mode is well

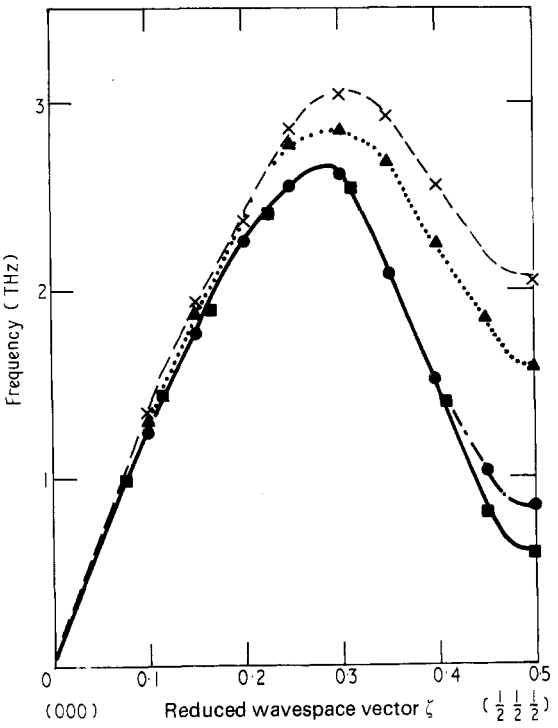

Figure 7. The [ζζζ] TA phonon dispersion curves of $KCoF_3/KMnF_3$ alloys at room temperature. The wavevector is that appropriate to the chemical Brillouin zone. Crosses, $KCoF_3$; triangles, $K(Co_{0.72}Mn_{0.28})F_3$; circles, $K(Co_{0.20}Mn_{0.80})F_3$; squares, $KMnF_3$.

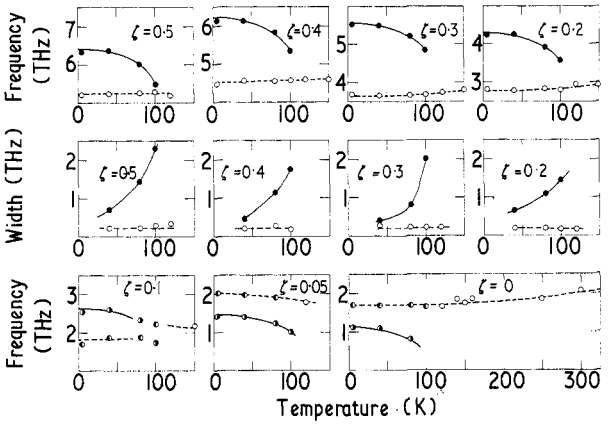

Figure 8. Frequencies and widths (fwhm) of neutron groups observed from $KCoF_3$ at wavevector transfers $\boldsymbol{Q} = (0{\cdot}5, 0{\cdot}5, 1{\cdot}5 + \zeta)2\pi/a$ as a function of temperature. Full (open) circles show excitations of a predominantly magnetic (phonon) character and half full circles denote excitations of mixed character. The curves are drawn as a guide to the eye. Full (broken) curves denote modes of predominantly magnetic (phonon) character.

established. For $\zeta = 0{\cdot}1, 0{\cdot}05$ and $0{\cdot}0$ the frequencies of both the upper and the lower modes are temperature dependent in varying degrees indicating that both modes are of mixed magnon and phonon character. The results shown in figure 8 indicate that the magnon–phonon interaction is appreciable only within a radius of approximately $0{\cdot}2 \times 2\pi/a$ of the centre of the magnetic Brillouin zone. As an illustration of the remarkable change with temperature of the character of the modes in this magnon–phonon interaction region, we show in figure 9 the scattered neutron distribution observed at $\zeta = 0{\cdot}1$ ($\boldsymbol{Q} = (0{\cdot}5, 0{\cdot}5, 1{\cdot}6)2\pi/a$) at several temperature.

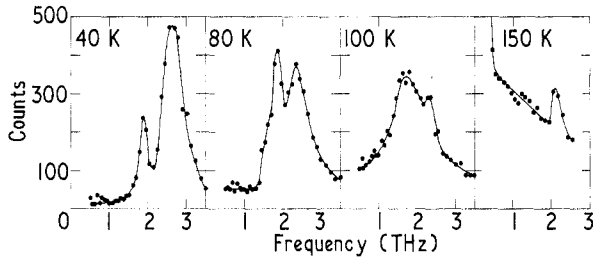

Figure 9. Scattered neutron distribution for $\boldsymbol{Q} = (0{\cdot}5, 0{\cdot}5, 1{\cdot}6)2\pi/a$ as a function of temperature. The groups have been normalized so that the same number of neutrons was incident on the specimen at each temperature. At 40 K the lower mode is predominantly phonon. When the temperature is raised to 80 K both modes have magnetic character and at higher temperatures the upper mode becomes predominantly phonon.

At the magnetic zone centre the slight decrease in frequency of the upper mode as the temperature increases in the antiferromagnetic phase is followed by a definite increase with increasing temperature in the paramagnetic phase amounting to about 10% between 120 and 300 K. A temperature dependent Γ_{25} mode is associated with antiferroelectricity in several perovskites but it has been shown to be too small to lead to an antiferroelectric transition at the cobalt rich end of the series $KMn_xCo_{1-x}F_3$ (Buyers *et al.* 1970).

3.5. *High-frequency magnetic modes*

In figure 4 it is seen that in addition to the low frequency magnetic excitations there are also excitations in the frequency range 9–10·3 THz. Typical examples of the scattering observed in this frequency range at various positions in reciprocal space and at different temperatures are shown in figure 10. It was found that the frequency of any particular one of these high frequency modes remained surprisingly constant as the temperature was raised. The intensity decreased however, and above T_N the sharp peaks observed at low temperatures had in many cases become so weak as to be unobservable, although for others a measurable intensity persisted. At low temperatures, the intensity of these modes exhibited a very strong wavevector dependence. The modes were also more intense in zones containing nuclear reciprocal lattice points than in those containing magnetic points. In fact no modes could be observed very near to magnetic reciprocal lattice points.

These modes are clearly associated with the magnetic properties of the crystal because of their rapid variation of intensity with temperature. Their constant frequency might have suggested that they were phonons seen via magnetovibrational scattering but this is thought to be unlikely. The intensity varies with wavevector more rapidly than would be expected for a phonon mode exhibiting little dispersion. The weak peaks observed above T_N for some of the scans would not be expected from magnetovibrational scattering and finally no flat phonon modes are known to occur in $KCoF_3$ in this frequency range (table 1). Although the possibility of magnetovibrational scattering cannot be completely ruled out it seems more likely that the scattering is associated with the magnetic transition from the

$j^z = \frac{1}{2}$ ground state to the lowest $j^z = \frac{3}{2}$ state. The lack of temperature variation in the observed frequency is explained by the energy level diagram, figure 2.

As the temperature is increased the exchange field is reduced from its low temperature value but since the separation of the lowest $j^z = \frac{1}{2}$ and $j^z = \frac{3}{2}$ level is approximately independent of the exchange field, the excitation frequency stays approximately constant. Above T_N other transitions from the ground doublet to the excited spin–orbit states will be exchange broadened with the result that the transition between $j^z = \frac{1}{2}$ and $j^z = \frac{3}{2}$ may be expected to appear as a discrete line superposed on a broad background. As the population of the ground state $j^z = \frac{1}{2}$ decreases as the temperature increases the intensity of this transition will decrease by approximately a factor two, which is not inconsistent with experiment.

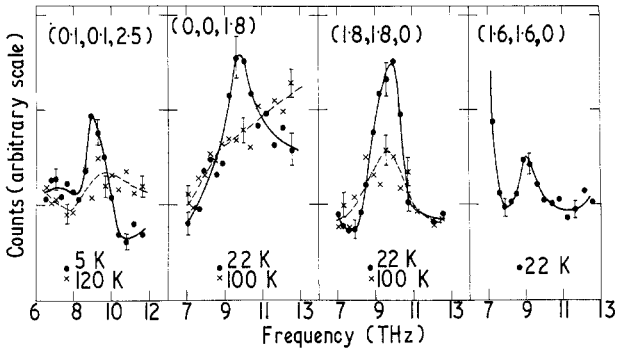

Figure 10. Scattered neutron distributions obtained in 'constant $\boldsymbol{Q}$' experiments corresponding to the high frequency magnetic excitations in $KCoF_3$. The bracketed quantities denote the positions in reciprocal space at which the measurements were made. The groups have been normalized so that the same number of neutrons were incident on the specimen in each case. Typical error limits are shown.

A final proof of the magnetic nature of the high frequency modes is that the magnetic structure factor calculated from a model involving transitions to all excited states of the $^4T_1$ orbital level is in good agreement with experiment (figure 5 of II). The strong scattering from the high frequency modes in nuclear zones and the weak scattering in magnetic zones results from the mixing of the $j^z = \frac{1}{2}$ and $j^z = \frac{3}{2}$ states by the transverse components of the exchange.

In certain regions of reciprocal space the modes exhibit rather rapid linewidth variations with wavevector transfer. This may indicate that there are other weaker modes participating in the scattering in the high frequency range; in particular, the observed scattering at some wavevectors may contain a contribution from the LO phonon, which has a frequency of 8·8 THz at the zone centre (table 1).

4. Summary

Dispersion relations for magnons, phonons and modes of mixed character have been measured in $KCoF_3$ by means of neutron inelastic scattering techniques. In addition to the magnetic modes associated with the transition between the members of the ground doublet of the Co^{2+} ion, a second branch of the magnon dispersion relation has been observed which corresponds to transitions from the ground state to the lowest state associated with the $j^z = \frac{3}{2}$ spin–orbit level. The absence of double neutron groups associated with the magnon scattering shows that any effect of directional anisotropy in the exchange is less than 8% in frequency.

The magnons in $KCoF_3$ have both spin and orbital angular components and are, therefore, sensitive to the fluctuating crystalline electric field produced by lattice vibrations. We

believe that this is the origin of the magnon–phonon interaction observed near the magnetic zone centre for the magnon branch of lowest frequency. The extent in wavevector of the interaction has been obtained from the temperature dependence of the magnon branch and the strength of the interaction was found to be 0·35 ± 0·10 THz.

The frequency of the upper of the two magnon branches studied was found to be temperature independent but its intensity decreased rapidly as the temperature was raised. This is qualitatively expected for this transition since it is practically independent of the magnitude of the exchange field. Our results show that the qualitative behaviour of magnons in crystals whose ions have unquenched orbital angular momentum in addition to spin can be quite different from magnons in crystals whose ions have only spin.

Acknowledgments

We wish to acknowledge E. A. Glaser, R. Campbell and H. Nieman of Chalk River Nuclear Laboratories for invaluable technical assistance. We wish to thank R. J. Elliott and M. F. Thorpe for useful discussions and we are grateful to T. G. Phillips for communicating his results prior to publication. M. T. H. would like to acknowledge the support of the Science Research Council and also the use of facilities and the help of technical staff at AERE, Harwell. He would like to thank M. F. Collins, D. H. Saunderson and C. G. Windsor for helpful discussions.

References

ANDERSON, P. W., 1963, *Solid St. Phys.*, **14**, 99–214.
AXE, J. D., and PETTIT, G. D., 1967, *Phys. Rev.*, **157**, 435–7.
BROCKHOUSE, B. N., 1961, *Inelastic Scattering of Neutrons in Solids and Liquids* (Vienna: International Atomic Energy Agency), pp. 113–51.
BUYERS, W. J. L. *et al.*, 1968, *Proc. 11th Int. Conf. Low Temp. Phys.* (St. Andrews: St. Andrews University Press), pp. 1330–5.
BUYERS, W. J. L., COWLEY, R. A., and PAUL, G. L., 1970, *J. Phys. Soc. Japan*, **28**, Suppl., 242–4.
BUYERS, W. J. L., *et al.*, 1971, *J. Phys.* C: *Solid St. Phys.*, **4**, 2139–59.
COLLINS, M. F., 1964, *Proc. Int. Conf. on Magnetism, Nottingham* (London: Institute of Physics and Physical Society), pp. 319–21.
COWLEY, R. A., 1964, *Phys. Rev.*, **134**, A981–5.
DYER, R. F., and LOW, G. G., 1961, *Inelastic Scattering of Neutrons in Solids and Liquids* (Vienna: International Atomic Energy Agency), pp. 179–94.
ELLIOTT, R. J., and THORPE, M. F., 1968, *J. appl. Phys.*, **39**, 802–7.
FERGUSON, J., WOOD, D. L., and KNOX, K., 1963, *J. chem. Phys.*, **39**, 881–9.
HUTCHINGS, M. T., RAINFORD, B. D., and GUGGENHEIM, H. J., 1970a, *J. Phys.* C: *Solid St. Phys.*, **3**, 307–22.
HUTCHINGS, M. T., *et al.*, 1970b, *Phys. Rev.* B. **2**, 1362–73.
KITTEL, C., 1963, *Quantum Theory of Solids* (New York: John Wiley), p. 74.
MARTEL, P., COWLEY, R. A., and STEVENSON, R. W. H., 1968, *Can. J. Phys.*, **46**, 1355–70.
MINKIEWICZ, V. J., and SHIRANE, G., 1969, *J. Phys. Soc. Jap.* **26**, 674–80.
NAGAI, O., and YOSHIMORI, A., 1961, *Prog. theor. Phys.*, **25**, 595–602.
OKAZAKI, A., and SUEMUNE, Y., 1961, *J. Phys. Soc. Japan*, **16**, 671–5.
OKAZAKI, A., TURBERFIELD, K. C., and STEVENSON, R. W. H., 1964, *Phys. Lett.*, **8**, 9–11.
PERRY, C. H., and YOUNG, E. F., 1967, *J. appl. Phys.*, **38**, 4616–24.
PICKART, S. J., COLLINS, M. F., and WINDSOR, C. G., 1966, *J. appl. Phys.*, **37**, 1054–5.
SAKURAI, J., BUYERS, W. J. L., COWLEY, R. A., and STEVENSON, R. W. H., 1968, *Phys. Rev.*, **167**, 510–8.
SAMUELSON, E. J., HUTCHINGS, M. T., and SHIRANE, G., 1970, *Physica*, **48**, 13–42.
SAMUELSON, E. J., and SHIRANE, G., 1970, *Phys. Stat. Solidi.*, **42**, 241–56.
SCATTURIN, V., CORLISS, L., ELLIOT, N. and HASTINGS, J., 1961, *Acta. Crystallogr.*, **14**, 19–26.
SVENSSON, E. C., *et al.*, 1969, *Can. J. Phys.*, **47**, 1983–8.
VAN VLECK, J. H., 1932, *The Theory of Electric and Magnetic Susceptibilities* (London: Oxford University Press), chap. XII.
WINDSOR, C. G., and STEVENSON, R. W. H., 1966, *Proc. Phys. Soc.*, **87**, 501–4.